Earthq Eng & Eng Vib (2023) 22: 117-134 **DOI**: https://doi.org/10.1007/s11803-023-2157-0

Selection and modification of ground motion records using Newmark-Hall spectrum as target spectrum for long-period structures

Fu Jianyu[1†], Wang Dongsheng[1‡], Zhang Rui[2§] and Chen Xiaoyu[3†]

1. *School of Civil and Transportation Engineering, Hebei University of Technology, Tianjin 300401, China*
2. *School of Civil Engineering, Dalian Jiaotong University, Dalian 116028, China*
3. *Institute of Road and Bridge Engineering, Dalian Maritime University, Dalian 116026, China*

Abstract: Input ground motions have significant impacts on the uncertainty of structural responses in time-history analysis. In this study, records were selected and scaled for the evaluation of mean structural responses according to the target spectrum. The Newmark-Hall spectrum is closely related to seismic response of short, medium and long-period structures, so it was taken as the target spectrum here. The nonlinear time-history analyses of 9-story and 20-story steel moment-resisting frame structures were carried out as examples. They represent medium and long-period buildings, respectively. Three target spectra with risk of 50%, 10% and 2% probabilities for exceedance in 50 years were calculated by the average Newmark-Hall spectrum method for three ground motion sets developed in the SAC Steel Project. The predicted structural mean responses of these Newmark-Hall spectra were compared with those calculated by the average spectral acceleration method for the same record set. It is found that both methods have similar accuracy for estimating the structural mean response. However, the method proposed herein is more effective in reducing the variability of the structural responses. Also, the proposed method is more advantageous for the time-history analysis of long-period structures or structures with more severe nonlinear responses under strong seismic excitations.

Keywords: time-history analysis; selection and modification of ground motions; target spectrum; Newmark-Hall spectrum; steel moment resisting frame structure

1 Introduction

The nonlinear time-history analysis is a widely accepted method for seismic design and assessment of structures, e.g., high-rise buildings and large-span bridges. According to the seismic codes, the nonlinear time-history analysis is the most commonly used process used process for performance-based design (Bommer and Acevedo, 2004). In general, the analyses of structural dynamic response present unacceptable variability when several random records are used as inputs (Padgett and Desroches, 2007; Katsanos *et al.*, 2010; Katsanos and Sextos, 2017). Therefore, an appropriate method for ground motion selection and modification should be adopted to reduce the bias and dispersion in the structural time-history analysis. In other words, a few scaled records should be used to accurately predict the structural mean responses with reduced record-to-record variability (Reyes *et al.*, 2014).

Since the 1990s, various methods have been developed to solve the complex problem of selecting and scaling earthquake records (PEER GMSM Working Group, 2009; Marasco and Cimellaro, 2017; Mergos and Sextos, 2019; Lombardi *et al.*, 2019; Moschen *et al.*, 2019; Theophilou, 2018). Among various methods, spectral matching is the most widely used in recent decades (Reyes *et al.*, 2014). Also, for structural analysis, the set of records, whose earthquake spectra values are compatible with the predefined target spectrum, can be considered as the optimal input ground motions. Therefore, defining the target spectrum is a critical point for selecting and scaling earthquake records.

The uniform hazard spectrum (UHS) is a prevalent alternative target spectrum derived from the probabilistic seismic hazard analysis (PSHA) for a specific site (Cornell, 1971; McGuire, 2004). UHS assumes an equal probability of exceedance for the spectral accelerations during the entire structural period range. However, the spectral values at each period are unlikely to occur simultaneously in a single earthquake (Malhotra, 2011).

Correspondence to: Wang Dongsheng, School of Civil and Transportation Engineering, Hebei University of Technology, Tianjin 300401, China
Tel: +86-22-60435950
E-mail: dswang@hebut.edu.cn
†PhD Candidate; ‡Professor; §Associate Professor

Supported by: National Natural Science Foundation of Hebei Province under Grant No. E2020202038, and the National Natural Science Foundation of China under Grant No. 51778206
Received January 19, 2021; **Accepted** March 4, 2022

Baker (2011) realized the limitation of UHS and then proposed the "conditional mean spectrum" (CMS), which can account for correlations among spectral accelerations for all periods. CMS is conditioned on the occurrence of a target spectral acceleration value at the period of interest. It utilizes an epsilon parameter (ε) that reflects the spectral shape and closely correlates with the structural response under real ground motions (Baker and Cornell, 2006; Haselton, 2009; Baker, 2011; Baker and Lee, 2017). Thus, CMS has attracted extensive attention and has been used in many applications (Mahmoud, 2008; Wang, 2015) because it can accurately estimate nonlinear structural responses (PEER GMSM Working Group, 2009) of multi-degree-of-freedom (MDOF) structures. However, for long-period structures, the responses are significantly influenced by multiple vibration modes. Also, CMS cannot realize that the spectral accelerations at these mode periods have an equal probability of exceedance. Thus, CMS may not be conservative for several structural response quantities (Carlton and Abrahamson, 2014; Kwong and Chopra, 2017). Note that, in the present study, the above-mentioned target spectra are performed on spectral accelerations to have a better correlation with the dynamic responses of short-period and/or medium-period structures. However, for long-period structures, such as high-rise buildings and large-span bridges, spectral accelerations may not be the optimal choice for the target spectra; instead, displacement response spectra is usually the better choice. Therefore, Chen *et al.* (2018) proposed a selection and scaling records methods which can match multiple target spectrum, including acceleration and displacement response spectra.

During the 1970s, Newmark and Hall (1969) found that for relatively low frequencies, the maximum displacement response is almost equal to the peak ground displacement (PGD). Also, they found that for high frequencies, the maximum acceleration response is equal to the peak ground acceleration (PGA). In addition, they found that for medium frequencies, the maximum response is more affected by the peak ground velocity (PGV). In fact, some studies indicated that the structural responses are correlated with the ground motion intensity measures (IMs). Zhang *et al.* (2017) identified and compared the correlation between 19 IMs and the maximum inter-story drift ratios of two super high-rise buildings, e.g., 61-story and 118-story buildings. Note that in the study of Zhang *et al.* (2017), most IMs considered the multiple modes of structures. They proposed a spectral velocity-based IM with superior sensitivity to the structural responses of super high-rise buildings. In their work, a decrease in the variation of structural seismic demands can be achieved by the combination of peak ground motion parameters, such as PGA, PGV, and PGD, and spectral responses. Riddell and Garcia (2001) and Riddell (2007) identified the correlation between the deformation demands and the energy response of single-degree-of-freedom (SDOF) systems and 23 IMs. They found that these IMs failed to show any satisfactory correlations with the system's displacement responses or hysteretic energy in all three spectral regions simultaneously. In other words, IMs developed from PGA, PGV, and PGD are sensitive to the short, medium, and long-period structural responses, respectively. Based on spectrum amplification factors in different sensitive regions of PGA, PGV, and PGD, Newmark and Hall (1982) proposed a smooth elastic design spectrum called the Newmark-Hall spectrum. This spectrum has a natural and perfect correlation with the short, medium, and long-period structural responses. To date, the Newmark-Hall spectrum has been widely used in many building standards (ASCE 4-98, 2000; CSA, 2010). Also, some related deeper insights were provided for deriving the design spectrum combined spectral accelerations versus spectral displacements (Calvi *et al.*, 2018).

However, in the past, it was not easy to accurately obtain PGD because the acquisition of real ground motions and the backward processing technology of earthquake records were limited. Thus, the development and application of the Newmark-Hall spectrum were limited. Fortunately, in recent years, a huge number of real strong-motion records have been significantly obtained around the world. Moreover, the technology for recording and processing earthquake ground motions has been developed together with global position systems (GPSs) so that the accurate acquisition of PGD has become available. In addition, the Next Generation Attenuation (NGA) project of Pacific Earthquake Engineering Research Center (PEER) has proposed a new empirical ground motion model for PGA, PGV, PGD, and 5% damped linear elastic response spectra (Campbell and Bozorgnia, 2008). The above-mentioned factors can help develop and modify the Newmark-Hall spectrum satisfactorily (Li *et al*., 2016; Palermo *et al.*, 2014) so that it can be considered as the target spectrum for structural time-history analysis.

This study aims to develop a selection and modification method for conventional earthquake ground motions. This method will be applicable in all short, medium, and long-period structures. Therefore, the Newmark-Hall spectrum, plotted by four logarithmic scales, is regarded as the target spectrum. A preliminary evaluation of the ground motion selection and scaling method with the target spectrum of the Newmark-Hall spectrum (N-HM) is conducted through the nonlinear time-history analysis of two tall buildings. The method using a Newmark-Hall spectrum as a target spectrum is denoted by N-HM. These buildings are 9-story and 20-story steel moment-resisting frame structures, representing medium and long-period structures, respectively. During spectral matching, the least squares method is used to quantify the residuals between the record′s scaled spectrum and target spectrum. Then, it will be shown that when the Newmark-Hall spectrum is taken as the target spectrum, the scale factors of the

records are mainly affected by the velocity-sensitive regions of the 9-story and 20-story structures.

2 Target Newmark-Hall spectrum for time-history analysis

2.1 Description of the spectrum

For the structure of a single-degree-of-freedom (SDOF) with a period of T, the spectral displacement response is $S_d(T)$. The pseudo-velocity response spectrum $PS_v(T)$ and the pseudo-acceleration response spectrum $PS_a(T)$ can be determined by Eqs. (1) and (2).

$$PS_v(T) = \omega S_d(T) \tag{1}$$

$$PS(T) = \omega^2 S(T) \tag{2}$$

where ω is the structural natural circular frequency equal to $\omega = \frac{2\pi}{T}$.

$PS_a(T)$, $PS_v(T)$, and $S_d(T)$ can be plotted by four logarithmic scales named as tripartite response spectra, and can be smoothed by the method proposed by Newmark and Hall (1982). The principle of smoothing and developing the Newmark-Hall design spectrum are illustrated in Fig. 1.

For a specified ground motion, the El Centro record is taken as an example, which is shown in Fig. 1. As can be seen, the pseudo-velocity response spectrum is replaced by multiple lines of *a-b-c-d-e-f* in the four-way logarithmic plot. The spectra amplitudes for the acceleration-sensitive, velocity-sensitive, and displacement-sensitive frequency bands are calculated by the multiplication of acceleration-amplification factor α_A and PGA, the multiplication of velocity-amplification factor α_V and PGV, and the multiplication of displacement-amplification factor α_D and PGD, respectively. Note that Hall *et al.* (1976) for the corner periods recommended the values of T_a = 1/33 s, T_b = 1/8 s, T_e = 10 s, T_f = 33 s. Note that the values of the corner periods, T_c and T_d, are not constant, and they depend on the relationships between the spectral values of *b-c* (acceleration-sensitive), *c-d* (velocity-sensitive,) and *d-e* (displacement-sensitive). Also, to obtain T_c and T_d, the equal-area criterion is used between the pseudo-velocity response spectrum of the specified record and the smoothed Newmark-Hall spectrum.

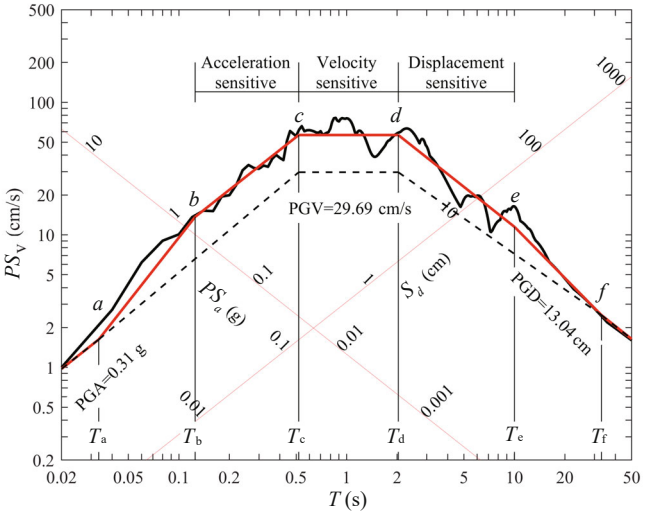

Fig. 1 Smoothed Newmark-Hall design spectrum for El Centro record with T_a = 1/33 s, T_b = 1/8 s, T_c = 0.52 s, T_d = 2.02 s, T_e = 10 s, T_f = 33 s, α_A = 2.23, α_V = 1.91, and α_D = 1.40

2.2 Definition of the target spectrum

Somerville *et al.* (1997) proposed three sets of ground motions assembled for the geographic locations in Los Angeles as a part of the SAC Steel Project. These sets of records were selected based on the probabilistic seismic hazard analysis (PSHA). They matched with the design response spectra defined in the National Earthquake Hazards Reduction Program (NEHRP 1994 (FEMA, 1997)) provisions. The three sets of records represented seismic hazard levels with the 50%, 10%, and 2% probabilities of exceedance in 50 years, respectively. It is worth mentioning that they were also referred to as 50/50, 10/50, and 2/50 sets or seismic hazard levels. Each set comprised 20 time histories, representing 10 ground motion stations with two orthogonal record components. Also, most sets are real earthquake records, but the record set of 2/50 seismic hazard level includes several simulated ground motions.

In the present study, the benchmark buildings of the 9-story and 20-story steel moment-resisting frame structures of the SAC Phase II Steel Project are used for the time history analysis (Ohtori *et al.* 2004). Not only the three record sets are used to build the target spectra, but also the average structural responses under these three record sets are defined as the benchmark mean demands. The pseudo-velocity response spectrum from each record has to be smoothed to the Newmark-Hall spectrum (the principle of smoothing is illustrated in Fig. 1). Then, the average smoothed Newmark-Hall spectrum from each set of records is defined as the target spectrum for various seismic hazard levels (Fig. 2). The damping ratio of these pseudo-velocity response spectra is 2%, which is consistent with that of the analyzed structures. Detailed properties of the structures are described in Section 3.1.

2.3 Scaling method of ground motions

The residuals between the record′s scaled spectrum and the target spectrum are minimized between T_m and $1.5T_1$ using the least squares method, which can minimize the scaling factor of each record. m is the

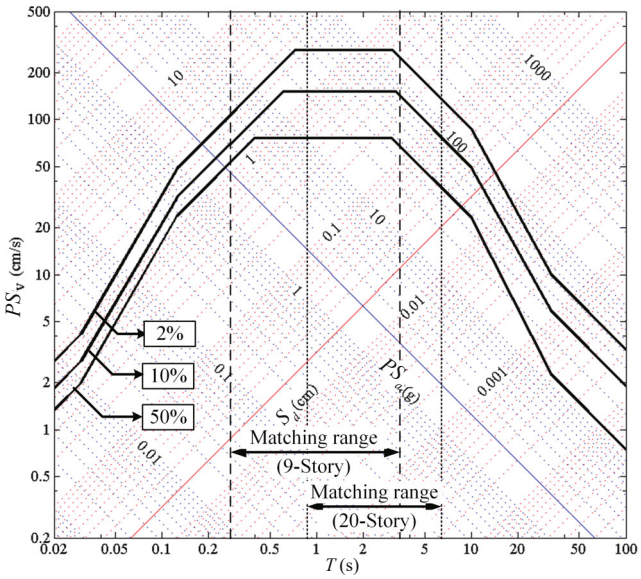

Fig. 2 Target Newmark-Hall spectrum at 50/50, 10/50, and 2/50 hazard levels, $\xi = 2\%$

number of vibration modes, which can ensure that the cumulative modal mass participation ratio is greater than 90% (Beyer and Bommer 2007; Katsanos and Sextos 2017), considering the effects of the higher mode for the structural responses. According to ASCE 7–10 (ASCE 2010), the upper bound is $1.5T_1$.

When the Newmark-Hall spectrum is defined as the target spectrum, the period ranging from T_m to $1.5T_1$ must cover two or three sensitive regions in the spectrum. Therefore, the residuals (SSE_N) should be the sum of squared errors calculated using PS_a, PS_v, and S_d in spectral acceleration, velocity, and displacement-sensitive regions, respectively. Thus, SSE_N is calculated as:

$$SSE_N = \sum_{T_i=T_m}^{T_c}\left[\ln SF\cdot PS_a(T_i)-\ln PS_a^t(T_i)\right]^2 + \sum_{T_i=T_c}^{T_d}\left[\ln SF\cdot PS_v(T_i)-\ln PS_v^t(T_i)\right]^2 + \sum_{T_i=T_d}^{1.5T_1}\left[\ln SF\cdot S_d(T_i)-\ln S_d^t(T_i)\right]^2 \quad (3)$$

where $PS_a(T_i)$, $PS_v(T_i)$, and $S_d(T_i)$ are the record's unscaled spectral acceleration, spectral velocity, and spectral displacement based on the Newmark-Hall spectrum. Also, their counterparts for the Newmark-Hall target spectrum are $PS_a^t(T_i)$, $PS_v^t(T_i)$, and $S_d^t(T_i)$, respectively. T_c and T_d are the corner periods for the target spectrum or the record's spectrum, and SF is the linear scaling factor of the record.

Equation (3) can also be described into Eq. (4) and its three parts have no units, so the various units in $PS_a(T_i)$, $PS_v(T_i)$, and $S_d(T_i)$ have no effects on the residuals (SEE_N).

$$SSE_N = \sum_{T_i=T_m}^{T_c}\left[\ln\left(\frac{SF\cdot PS_a(T_i)}{PS_a^t(T_i)}\right)\right]^2 + \sum_{T_i=T_c}^{T_d}\left[\ln\left(\frac{SF\cdot PS_v(T_i)}{PS_v^t(T_i)}\right)\right]^2 + \sum_{T_i=T_d}^{1.5T_1}\left[\ln\left(\frac{SF\cdot S_d(T_i)}{S_d^t(T_i)}\right)\right]^2 \quad (4)$$

Nevertheless, corner periods T_c or T_d are usually different between the target spectrum and the records. Thus, SSE_N is not easy to calculate by Eq. (3). Fortunately, $PS_a(T)$, $PS_v(T)$, and $S_d(T)$ are related to each other by the structural natural circular frequency (ω) as shown in Eq. (5).

$$PS_a(T) = \omega PS_v(T) = \omega^2 S_d(T) \quad (5)$$

When Eq. (5) is substituted into Eq. (3), and SSE_N is rewritten, then Eq. (6) can be obtained; it only includes the pseudo-velocity response spectrum. Thus, the calculation becomes easier.

$$SSE_N = \sum_{i=1}^{n}\left[\ln(SF\cdot PS_v(T_i)) - \ln PS_v^t(T_i)\right]^2 \quad (6)$$

where the parameters have the same definitions as in Eq. (3), and $PS_v^t(T_i)$ is the target Newmark-Hall spectrum at period T_i. As shown in Eq. (7), SF is the scaling factor by which SSE_N is minimized by setting the derivative to zero, i.e., $\mathrm{d}SSE_N/\mathrm{d}SF \cong 0$.

$$\ln SF = \frac{1}{n}\sum_{i=1}^{n}\left[\ln PS_v^t(T_i) - \ln PS_v(T_i)\right] \quad (7)$$

2.4 Ground motions for selection

In recent years, several strong-motion databases, which make real earthquake records more accessible in structural time-history analysis, have been greatly developed. Therefore, in the present study, only real records are selected and scaled. Table 1 shows that the selection and scaling of real records, which are 40 components, are carried out from 20 stations with two orthogonal components in the PEER NGA databank.

Except for I-ELC180, I-ELC270, TAF021, and TAF111, the components in Table 1 are all different from that proposed in ground motion sets in the SAC project (Somerville, 1997). The records are from six earthquake events and selected following the simple rules of Miranda and Ruiz-Garcia (2001) as: ① moment magnitude (M_w) is greater than or equal to 6, ② fault rupture distance (dR_{up}) is in the range of 20–40 km, and the near-fault ground motions are removed, ③ site conditions (NEHRP 1994) are assumed as soft-rock (site

class C), and stiff soil (site class D), and V_{s30} is in the range of 180–760 m/s, ④ PGA is greater than or equal to 0.15 g, and ⑤ the lowest useable frequency, less than or equal to 0.2 Hz, is assumed. Note that these rules are determined based on the assumption that the ground motions can cause damage to the structures.

2.5 Selecting and grouping the records

For the 9-story and 20-story structures at three seismic hazard levels, Fig. 3 shows *SF*s of the 40 earthquake record components calculated by the N-HM method using Eq. (7). Note that the results are obtained

Table 1 20 stations with two-component ground motions

ID number	Component	Event	Station	M_w	dR_{up} (km)	PGA (g)	PGV (cm/s)	PGD (cm)
1	AND270	Loma Prieta (89/10/18)	1652 Anderson Dam	7.0	21.40	0.24	20.3	7.7
2	AND360					0.24	18.4	6.7
3	BLD090	Northridge (94/01/17)	24157 LA - Baldwin Hills	6.7	31.30	0.24	14.9	6.2
4	BLD360					0.17	17.6	4.8
5	CCN090	Northridge (94/01/17)	24389 LA - Century City	6.7	25.75	0.26	21.1	6.7
6	CCN360					0.22	25.2	5.7
7	CLW-LN	Landers (92/06/28)	23 Coolwater	7.3	21.20	0.28	25.6	13.7
8	CLW-TR					0.42	42.3	13.8
9	TCU047-N	ChiChi (99/09/20)	Tcu047	7.6	33.01	0.41	40.2	22.2
10	TCU047-W					0.30	41.6	51.1
11	TCU095-N	ChiChi (99/09/20)	Tcu095	7.6	43.44	0.71	49.1	24.5
12	TCU095-W					0.38	62.0	51.8
13	WST000	Northridge (94/01/17)	90021LA - N Westmoreland	6.7	29.00	0.40	20.9	2.3
14	WST270					0.36	20.9	4.3
15	TCU045-N	ChiChi (99/09/20)	Tcu045	7.6	24.06	0.50	39.0	14.3
16	TCU045-W					0.47	36.7	50.7
17	I-ELC180	Imperial Valley (40/05/19)	117 El Centro Array #9	6.9	8.30	0.31	29.8	13.3
18	I-ELC270					0.21	30.2	23.9
19	TAF021	Kern County (52/07/21)	1095 Taft Lin-coln School	7.7	41.00	0.16	15.3	9.2
20	TAF111					0.18	17.5	9.0
21	CHY036-N	ChiChi (99/09/20)	CHY036	7.6	20.38	0.21	41.4	34.2
22	CHY036-W					0.29	38.9	21.2
23	FAR000	Northridge (94/01/17)	90016 LA - N Faring Rd	6.7	23.90	0.27	15.8	3.3
24	FAR090					0.24	29.8	4.7
25	GLP177	Northridge (94/01/17)	90063 Glendale - Las Palmas	6.7	25.40	0.36	12.3	1.9
26	GLP267					0.21	7.4	1.7
27	HCH090	Loma Prieta (89/10/18)	1028 Hollister City Hall	7.0	28.20	0.25	38.5	17.8
28	HCH180					0.22	45.0	26.1
29	H-CHI012	Imperial Valley (79/10/15)	6621 Chihuahua	6.5	28.70	0.27	24.9	9.1
30	H-CHI282					0.25	30.1	12.9
31	STN020	Northridge (94/01/17)	90091 LA - Saturn St	6.7	30.00	0.47	34.6	6.5
32	STN110					0.44	39.0	6.4
33	SVL270	Loma Prieta (89/10/18)	1695 Sunnyvale - Colton Ave.	7.0	28.80	0.21	37.3	19.1
34	SVL360					0.21	36.0	16.9
35	TCU042-N	ChiChi (99/09/20)	TCU042	7.6	23.34	0.20	39.3	23.9
36	TCU042-W					0.24	44.8	46.9
37	TCU107-N	ChiChi (99/09/20)	TCU107	7.6	20.35	0.16	47.4	32.8
38	TCU107-W					0.12	36.8	39.8
39	YER270	Landers (92/06/28)	22074 Yermo Fire Station	7.3	24.90	0.25	51.5	43.8
40	YER360					0.15	29.7	24.7

by the conventional method that takes the acceleration spectrum with arithmetic values as the target spectrum (Kalkan and Chopra, 2010). The method using an acceleration spectrum as a target spectrum is denoted by A-SM. The residuals of A-SM are denoted by SSE_S. The A-SM methods can be found in Kalkan and Chopra (2010).

The *SF*s of the 9-story structure calculated by the N-HM method are larger than that calculated by the A-SM method for most of the components and at all three seismic hazard levels. For the 20-story structure, *SF*s calculated by the N-HM method are rather close to that obtained by the A-SM method at all three seismic hazard levels, except for components No. 25 and 26. Additionally, as shown in Figs. 4(c) and 4(f), there are few records of which *SF*s are very large; for example, GLP177 (ID: 25, SF = 7.21 and 18.73), GLP267 (ID: 26, SF = 8.50 and 25.83). Note that scaling factors exceeding 6–7 (or even less) are not adopted to scale records for time-history analysis. Thus, these heavily scaled motions are not selected and not used in the time-history analysis of these two buildings.

Figure 4 shows the relative errors of *SF*s of the 40 earthquake record components calculated by the N-HM and A-SM methods. The relative errors of the *SF*s are defined as the difference between the *SF*s by N-HM and the *SF*s by A-SM divided by the *SF*s by A-SM. The relative errors of *SF*s at three seismic hazard levels are rather close to each other for the same structure. Also, they are insensitive to the seismic hazard levels. Among all 40 components, the relative errors for the 9-story structure are almost positive, meaning that *SF*s calculated by the N-HM method are larger than those by the A-SM method. However, half of the components have negative relative errors for the 20-story structure. In other words, the relative errors for the 9-story structure are larger than those for the 20-story structure at the same hazard level. Note that the larger values in the target spectrum are more effective in determining SSE_S (SSE_N) and *SF*s. The matching period regions for the 9-story and the 20-story structure are marked in Fig. 2. It can be seen that SSE_S (SSE_N) and *SF*s for the 9-story structure mainly depend on the acceleration-sensitive region and the velocity-sensitive region, while for the 20-story structure, they depend on the velocity-sensitive region and the displacement-sensitive region. When the acceleration spectrum with linear coordinate is taken as the target spectrum, *SF*s of the 9-story structure

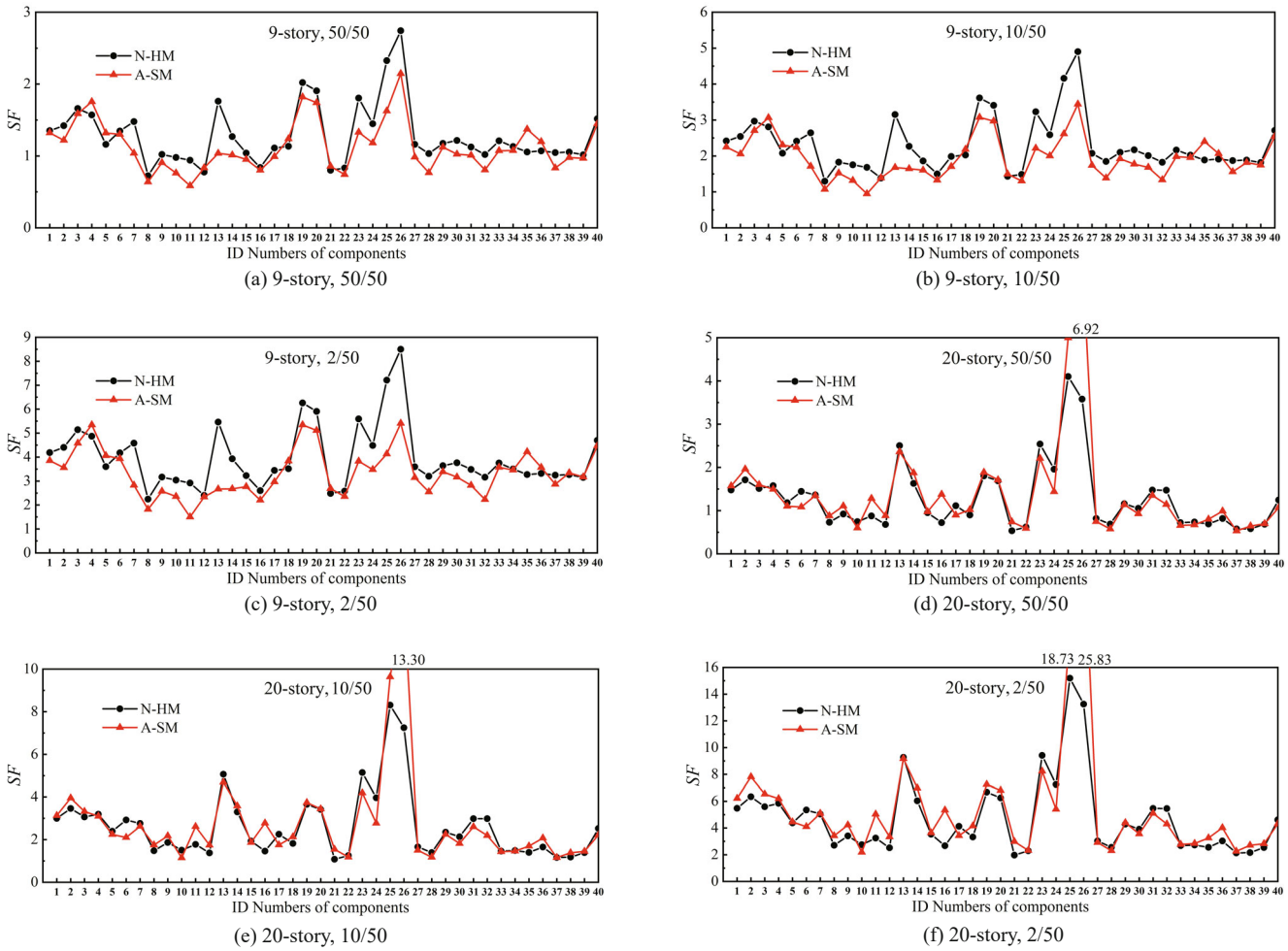

Fig. 3 Comparison of SFs calculated by N-HM and A-SM

with a fundamental period of 2.15 s (see Table 4) is influenced more by the acceleration-sensitive region, This is explained by the theory of vectors in (Zhang *et al.*, 2020) .When the Newmark-Hall spectrum is taken as the target spectrum, *SF*s of the 9-story structure are affected more by the velocity-sensitive region (Fig. 2). They result in the different *SF*s of the N-HM method and the A-SM method. However, for the 20-story structure, SSE_S (SSE_N) and *SF*s are both more dependent on the velocity-sensitive region when the acceleration and Newmark-Hall spectra are taken as the target spectrum. Thus, the differences of *SF*s from these two methods are more minor for the 20-story structure than those for the 9-story structure.

The number of records required for dynamic analyses significantly affects the estimation of the mean structural responses. In general, at least three records are required in some seismic codes (e.g., Eurocode 8 (CEN, EN 1998-3, 2005), ASCE 7–10 (2010), DOE (2002)). Shome *et al.* (1998) demonstrated that seven records are suitable to obtain acceptably low dispersive results. Reyes and Kalkan (2011) suggested that increasing the number of records from seven to 10 has a minor effect on the estimation accuracy of the structural response. However, if the statistical distribution of the structural responses or the probability of structural collapse is considered in the analysis, the required number of records can even be greater, i.e., at least 30 (Catalán *et al.*, 2010) or 60 (Wang, 2011).

The present study aims to investigate the difference between the structural mean response subjected to the records selected by the N-HM and A-SM methods. In addition, the present study aims to verify the feasibility selection of the Newmark-Hall spectrum as the target spectrum. Therefore, four different numbers of records, including 3, 7, 10, and 14, are adopted. Moreover, only one horizontal component of a station is selected to avoid the influence of the interdependency between both components recorded in the same station. The records with a minimum SSE_N (SSE_S), and with *SF* close to one have more priority of being selected for the time-history analysis of structures. Note that all 40 components are ranked according to the above-mentioned principles. The first 14 components selected by the N-HM and A-SM methods at three seismic hazard levels for both buildings are listed in Tables 2 and 3, respectively. Note that the numbers in Tables 2 and 3 are the corresponding ID numbers in Table 1.

According to the principles, which are minimum SSE_N (SSE_S) and *SF* close to 1.0, the ranking process of the ground motions is not limited by strict qualitative parameters. Note that the components of six record stations have been removed because they have too large *SF* or *SSE* and thus are not suitable for time-history analysis. For the same building and at the same seismic hazard level, there are five to nine stations from which the one or two components of the records are selected by the N-HM and A-SM methods.

The ground motion groups using the N-HM method are referred to as $\bar{G}i$ ($i=3,\ 7,\ 10,\ 14$), and the groups using the A-SM method are referred to as $\bar{G}i$ ($i=3,\ 7,\ 10,\ 14$), where i represents the required number of record′s components in the group which includes the first to the ith ground motions in Tables 2 or 3.

The components in groups Gi and $\bar{G}i$ are not always the same, but all components in group Gi ($\bar{G}i$) are included in group $\bar{G}j$ ($\bar{G}j$) if $j>i$. The orders of sequence of the selected components in the same ground motion group have no effect on the results of the time-history analysis because the average responses of each building are considered under each group.

Figure 5 shows the average spectrum of $\bar{G}i$ ($i=3,\ 7,\ 10,\ 14$) and the target spectrum for the 20-story structure at the 2/50 hazard levels. The calculation for the smoothed average Newmark-Hall spectrum of $\bar{G}i$ ($i=3,\ 7,\ 10,\ 14$) is based on the suggestions of Newmark *et al.* (1973) and Li *et al.* (2006). The average spectrum of each group is similar with the target spectrum at the acceleration-sensitive and velocity-sensitive frequency bands but not at the displacement-sensitive frequency band.

3 Analysis of nonlinear structural response

3.1 Structural models

The 9-story and 20-story steel moment-resisting frame structures used in this study are designed for the SAC Phase II Steel Project (Ohtori *et al.*, 2004) assuming that it would be located in Los Angeles. In fact, the

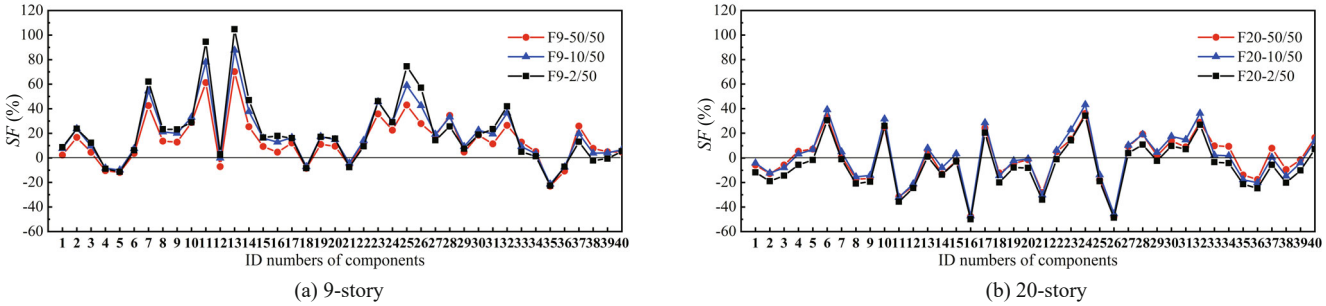

(a) 9-story (b) 20-story

Fig. 4 Comparison of the relative errors of SFs calculated by N-HM and A-SM

buildings are not constructed, but they still can represent typical medium and high-rise buildings in regions with high risk of earthquakes. The plan′s dimensions of 9-story and 20-story structures are 45.73 m × 45.73 m and 30.48 m × 36.58 m, and their heights are 37.19 m and 80.77 m, respectively. The lateral load-resisting systems of both buildings are comprised of steel-perimeter and moment-resisting frames. More detailed information is provided in the literature, e.g., Ohtori *et al.* (2004), Gupta and Krawinkler (1999), and Chopra (2004).

Table 2 Selected components for the 9-story structure at three seismic hazard levels

Sequence	50/50						10/50						2/50					
	N-HM			A-SM			N-HM			A-SM			N-HM			A-SM		
	ID*	*SF*	SSE_N	ID	*SF*	SSE_S	ID	*SF*	SSE_N	ID	*SF*	SSE_S	ID	*SF*	SSE_N	ID	*SF*	SSE_S
1	15	1.0	0.01	15	1.0	0.35	30	2.2	0.02	35	2.4	0.94	22	2.6	0.13	5	4.1	3.96
2	17	1.1	0.04	17	1.0	0.44	40	2.7	0.38	18	2.2	1.02	10	3.0	0.13	35	4.2	3.63
3	5	1.2	0.08	36	1.2	0.46	36	1.9	0.65	5	2.3	1.08	18	3.5	0.21	39	3.2	4.27
4	12	0.8	0.12	9	0.9	0.47	18	2.0	0.65	40	2.5	1.48	36	3.3	0.22	28	2.5	4.87
5	19	2.0	0.00	32	0.8	0.50	10	1.8	0.78	3	2.7	1.71	27	3.6	0.82	18	3.8	4.26
6	3	1.7	0.25	3	1.6	0.48	8	1.3	2.16	15	1.6	1.83	30	3.8	1.80	30	3.2	5.56
7	9	1.0	0.29	6	1.3	0.61	22	1.5	2.42	20	3.0	1.98	39	3.1	2.56	38	3.3	7.06
8	1	1.4	0.68	7	1.0	0.64	16	1.5	2.72	30	1.8	2.22	34	3.5	4.90	22	2.4	7.07
9	8	0.7	1.61	19	1.8	0.56	4	2.8	3.64	9	1.5	2.29	8	2.2	6.67	15	2.8	9.28
10	29	1.2	1.99	29	1.1	0.80	6	2.4	3.89	27	1.7	2.65	16	2.6	7.76	10	2.4	10.83
11	40	1.5	3.36	12	0.8	0.81	27	2.1	4.31	31	1.7	2.84	12	2.4	10.39	19	5.3	9.51
12	14	1.3	8.78	1	1.3	0.86	12	1.4	4.47	1	2.2	2.87	6	4.2	7.79	3	4.6	11.21
13	36	1.1	9.95	40	1.4	0.87	20	3.4	5.56	22	1.3	3.17	4	4.9	9.17	1	3.9	13.02
14	31	1.1	11.37	24	1.2	1.02	1	2.4	7.16	8	1.1	3.43	1	4.2	14.02	24	3.5	13.37

* The numbers are the corresponding ID numbers in Table 1.

Table 3 Selected components for the 20-story structure at three seismic hazard levels

Sequence	50/50						10/50						2/50					
	N-HM			A-SM			N-HM			A-SM			N-HM			A-SM		
	ID*	*SF*	SSE_N	ID	*SF*	SSE_S	ID	*SF*	SSE_N	ID	*SF*	SSE_S	ID	*SF*	SSE_N	ID	*SF*	SSE_S
1	17	1.1	0.03	36	1.0	0.58	21	1.1	6.35	28	1.2	0.52	21	2.0	7.59	28	2.3	2.06
2	30	1.1	0.61	15	1.0	0.19	18	1.8	1.95	10	1.1	2.34	8	2.7	1.18	22	2.3	5.78
3	5	1.2	0.03	18	1.0	0.41	30	2.1	0.20	37	1.2	2.32	30	3.9	0.53	38	2.7	5.58
4	4	1.6	0.22	30	0.9	0.12	12	1.4	5.83	22	1.2	1.50	12	2.5	7.02	39	2.8	4.24
5	15	1.0	3.11	6	1.1	0.13	39	1.4	6.32	39	1.4	0.95	39	2.5	7.56	10	2.2	11.50
6	40	1.2	7.27	40	1.1	0.42	28	1.4	6.46	34	1.5	3.32	28	2.5	7.71	34	2.8	13.62
7	9	0.9	7.27	9	1.1	0.19	35	1.4	6.73	35	1.7	2.75	18	3.3	2.74	17	3.4	4.95
8	7	1.4	6.90	32	1.1	0.16	5	2.4	0.25	8	1.7	1.63	35	2.6	8.01	8	3.4	6.69
9	11	0.9	5.51	8	0.9	0.32	16	1.5	5.83	17	1.8	1.16	16	2.7	7.02	30	3.6	4.65
10	27	0.8	7.39	12	0.9	0.50	34	1.5	6.99	12	1.7	2.43	10	2.8	7.02	11	5.0	5.70
11	36	0.8	7.27	27	0.7	0.19	8	1.5	1.82	30	1.8	1.10	34	2.7	8.28	15	3.6	8.64
12	1	1.5	2.87	21	0.7	0.77	37	1.2	15.85	15	1.9	2.05	37	2.1	17.59	36	4.0	6.12
13	34	0.7	8.55	24	1.4	0.20	10	1.5	5.83	6	2.1	1.49	5	4.4	0.05	6	4.1	6.33
14	20	1.7	7.27	34	0.7	1.25	1	3.0	4.04	32	2.2	1.92	1	5.5	3.05	32	4.3	7.36

* The numbers are the corresponding ID numbers in Table 1.

Two-dimensional (2D) structural finite element models (FEMs) are established based on the platform of ABAQUS 6.12 (2012). B22 elements are used to model the beams and columns. The bilinear material constitutive model with a strain-hardening ratio of 0.01 is applied to the steel material. Rayleigh damping with a damping ratio of 2% is used for the first and second vibration modes. Following Gupta and Krawinkler (1999), the shear behavior of the panel zone is also considered in FEMs.

For verification of the proposed structural models, the periods of the building models herein are compared with the results obtained by Ohtori *et al.* (2004); they are almost the same. Nonlinear time-history analysis is also carried out and the structural responses are consistent with (Gupta and Krawinkler, 1999), when the 50/50, 10/50, and 2/50 sets of ground motions proposed by the SAC project are used as inputs. More detailed information for verification of the proposed models can be found in (Zhang *et al.*, 2020)

Table 4 lists the lower three and four vibration periods of the 9-story and the 20-story structures and the modal-mass participation factors. The lower four modes must be considered for the 9-story structure, and the lower three modes should be considered for the 20-story structure.

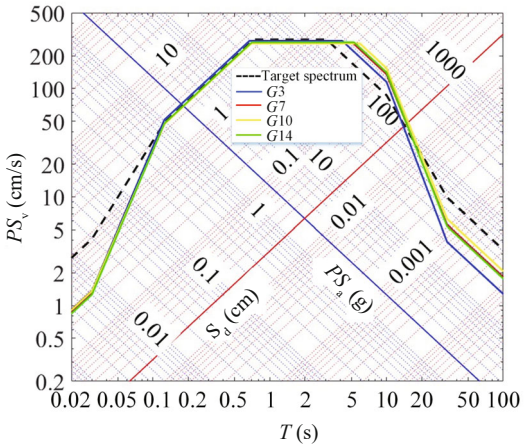

Fig. 5 Average spectrum of $\overline{Gi}$ (i = 3, 7, 10, 14) and target spectrum for the 20-story structure at 2/50 hazard levels

3.2 Structural response analysis

The arithmetic mean, which has been extensively specified by building codes (e.g., Eurocode 8 (CEN, EN 1998-3, 1997), ASCE 7–10 (2010)), is used to determine response design values. Thus, engineers are more familiar with the arithmetic mean for the response parameters adopted in the current study. Therefore, the average spectrum and the structural mean responses are all denoted by arithmetic means. The inter-story drift ratio, which is associated closely with structural damage (Miranda and Aslani, 2003), acts as a primary structural response parameter for performance-based earthquake engineering and structural specifications in many countries, e.g., Eurocode 8 (CEN, EN 1998-3, 1997), and ASCE 7–10 (2010). Therefore, the maximum inter-story drift ratios and the peak inter-story drift ratios over the height of the structures are taken as the engineering demand parameters (EDPs).

At the beginning of the analysis, the "true" structural responses, i.e., "benchmark mean demands" of the 9-story and 20-story structures, are determined under the earthquake excitations of the 50/50, 10/50, and 2/50 sets of ground motions proposed by the SAC project. It has been mentioned in Section 2.1 that the target spectrum is defined by the average spectrum from each set of these records, the smoothed Newmark-Hall spectrum, or the common acceleration spectrum.

3.2.1 Peak inter-story drift ratios over the heights of the structures

Figures 6 and 7 show the peak inter-story drift ratio (PIDR) demands over the height of the 9-story and 20-story structures at three seismic hazard levels. The PIDR demands calculated by both N-HM and A-SM methods have a similar distribution along the height of the structures. Also, the N-HM and A-SM methods have predicated the same weakest floor with the structural response. Note that the weakest floor is defined as the floor where the maximum inter-story drift ratio (MIDR) occurs among all the building floors. In the 9-story structure, the weakest floor is the eighth floor at 50/50 and 10/50 hazard levels and the fourth floor at the 2/50 hazard level. In the 20-story structure, the weakest floor

Table 4 Vibration periods of 9-story and 20-story structures

Model	Vibration mode	Periods (s)	Modal-mass participation factors	Cumulative modal mass participation factors
9-story	1st	2.15	0.731	0.731
	2nd	0.81	0.109	0.840
	3rd	0.45	0.044	0.884
	4rd	0.29	0.019	0.903
20-story	1st	4.11	0.755	0.755
	2nd	1.47	0.115	0.870
	3rd	0.86	0.038	0.908

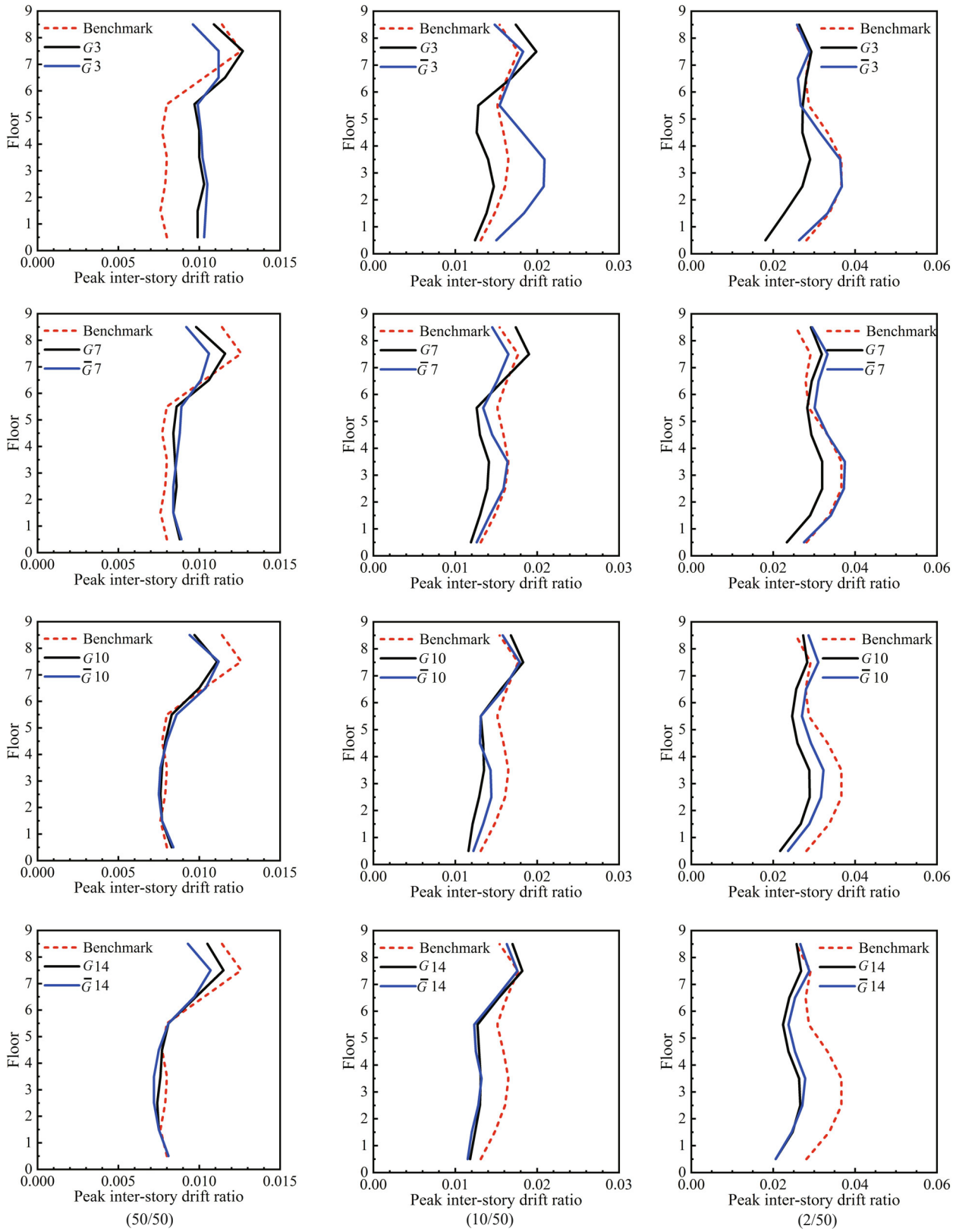

Fig. 6 PIDR demands over the height of the 9-story structure under ground motion groups *Gi* ($\bar{G}i$) (*i* = 3, 7, 10, 14) at 50/50, 10/50, and 2/50 hazard levels

is the eighteenth floor at the 50/50 hazard level and the third floor at the 10/50 and 2/50 hazard levels.

This study compares the effects of the N-HM and A-SM methods on the structural responses in time-history analysis. The PIDR demands under the groups *Gi* and $\bar{G}i$ (*i* = 7, 10, 14) are similar along the height of the structures at three seismic hazard levels. However, the demands of *G*3 and $\bar{G}3$ have some differences. The trend

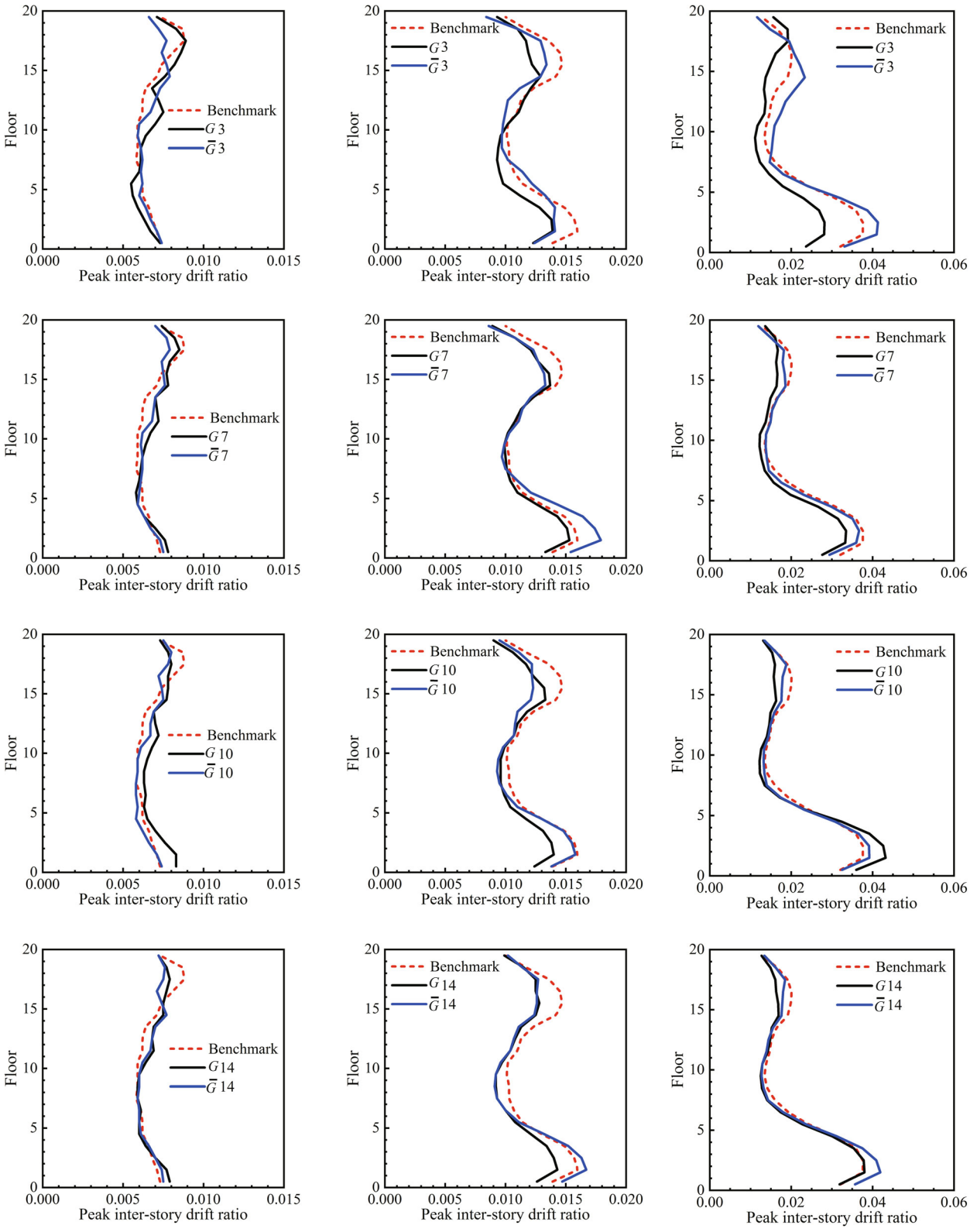

Fig. 7 PIDR demands over the height of the 20-story structure under ground motion groups *Gi* ($\bar{G}i$) (*i* = 3, 7, 10, 14) at 50/50, 10/50, and 2/50 hazard levels

is insensitive to the structural dynamic characteristics of either the 9-story or 20-story structure. Also, the trend is insensitive to the required number of records (7 or 10) and the nonlinear degree of the structural response.

For further clarification, the relative errors of the PIDR demands over the height of the structures are analyzed. The relative error is defined as the difference between the average EDPs of each ground motion group, *Gi* ($\bar{G}i$),

and the corresponding benchmark demands divided by the benchmark demands. In terms of the relative error, there are no obvious differences between the N-HM and A-SM methods, except for $G3$ and $\bar{G}3$. The maximum relative errors over the structure's height can be reduced by less than 20% (absolute value) if the optimal seven or ten records are selected. The error produced by both N-HM and A-SM methods for the 20-story building is less than that for the 9-story building.

Clearly, a more severe nonlinear response is undoubtedly produced at the higher seismic hazard levels. The pushover analyses for the two structures were carried out using the design load pattern suggested in FEMA 222A (1995). The global pushover plots, i.e., the normalized based shear (base shear normalized by structure seismic weight, or V/W) versus roof drift angle (roof relative displacement normalized by structural height from the column base pins) of the two structures is shown in Fig. 8. When the roof drift ratio is increased to 0.007, both structures almost show nonlinearity. Moreover, the mean peak roof drift ratios of the 9-story and 20-story structures under the records of $G7$ and $\bar{G}7$ at three seismic hazard levels are also plotted in Fig. 9. Both structures necessarily behave in a nonlinear manner under the seismic excitations of 10/50 and 2/50 seismic hazard levels.

The coefficient of variation (CV), defined as the ratio of the sample standard deviation and the sample mean, is used to assess the effectiveness (efficiency) of the N-HM method in reducing the dispersion of the structural response. Figure 9 shows CVs of the PIDR demands over the height of the 9-story structure for each ground motion group and various seismic hazard levels. There are insignificant differences between the N-HM and A-SM methods over the structure's height at 50/50 and 10/50 hazard levels. However, at the 2/50 hazard level, CVs of the N-HM method are not significant and less than those of the A-SM method.

Figure 10 shows CVs of the PIDR demands over the height of the 20-story structure at each seismic hazard level. CVs of both N-HM and A-SM methods are similar over the structure's height at the 50/50 hazard level. Nevertheless, the differences between CVs of both methods are remarkably increased at the lower floors from the first to fifth floors of the structure at 10/50 and 2/50 hazard levels. The CV value of $G14$ is 0.30 and the CV value of $\bar{G}14$ is 0.63 at the second floor for the 10/50 hazard level. However, at the 2/50 hazard level, the CV value of $G14$ is equal to 0.56, but the CV value of $\bar{G}14$ increases up to 0.89 at the second floor. CVs of the N-HM method are significantly less than CVs of the A-SM method at these lower floors for the 20-story structure, especially when the more severe nonlinear responses are produced. Note that CVs of the PIDR demands under the ground motion groups $G3$ and $\bar{G}3$ are not shown here because there are only three records.

The N-HM method is more advantageous in reducing the structural response variability than the A-SM method. In other words, the Newmark-Hall spectrum has a better correlation with the medium and long-period structural responses than the conventional acceleration spectrum. Also, the advantage is more obvious, especially for longer-period structures (20-story). In addition, the nonlinear response of the structure increases the structural period, which favors reducing the structural response variability if the Newmark-Hall spectrum is used as the target spectrum.

3.2.2 Maximum inter-story drift ratio

Figures 11 and 12 show the relative errors and CVs of the MIDR demands of the 9-story and 20-story structures under each record group at three seismic hazard levels. The MIDR demands have the same trends as the PIDR demands. The N-HM and A-SM methods have the same accuracy in predicting average MIDR demands. Moreover, the N-HM method can reduce the variability of MIDR demands more efficiently, especially for the 20-story structure when more severe nonlinear structural responses occur, i.e., for 10/50 and 2/50 seismic hazard levels.

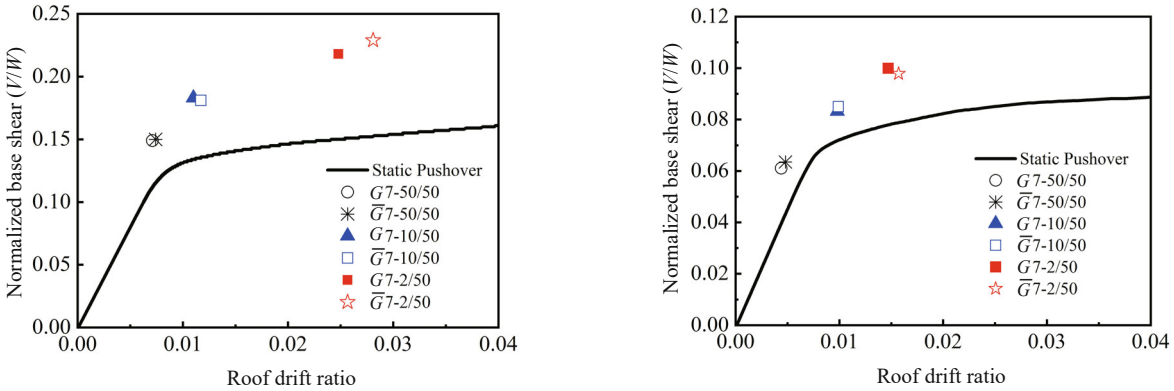

(a) 9-story (b) 20-story

Fig. 8 Global pushover curves for 9-story and 20-story structures

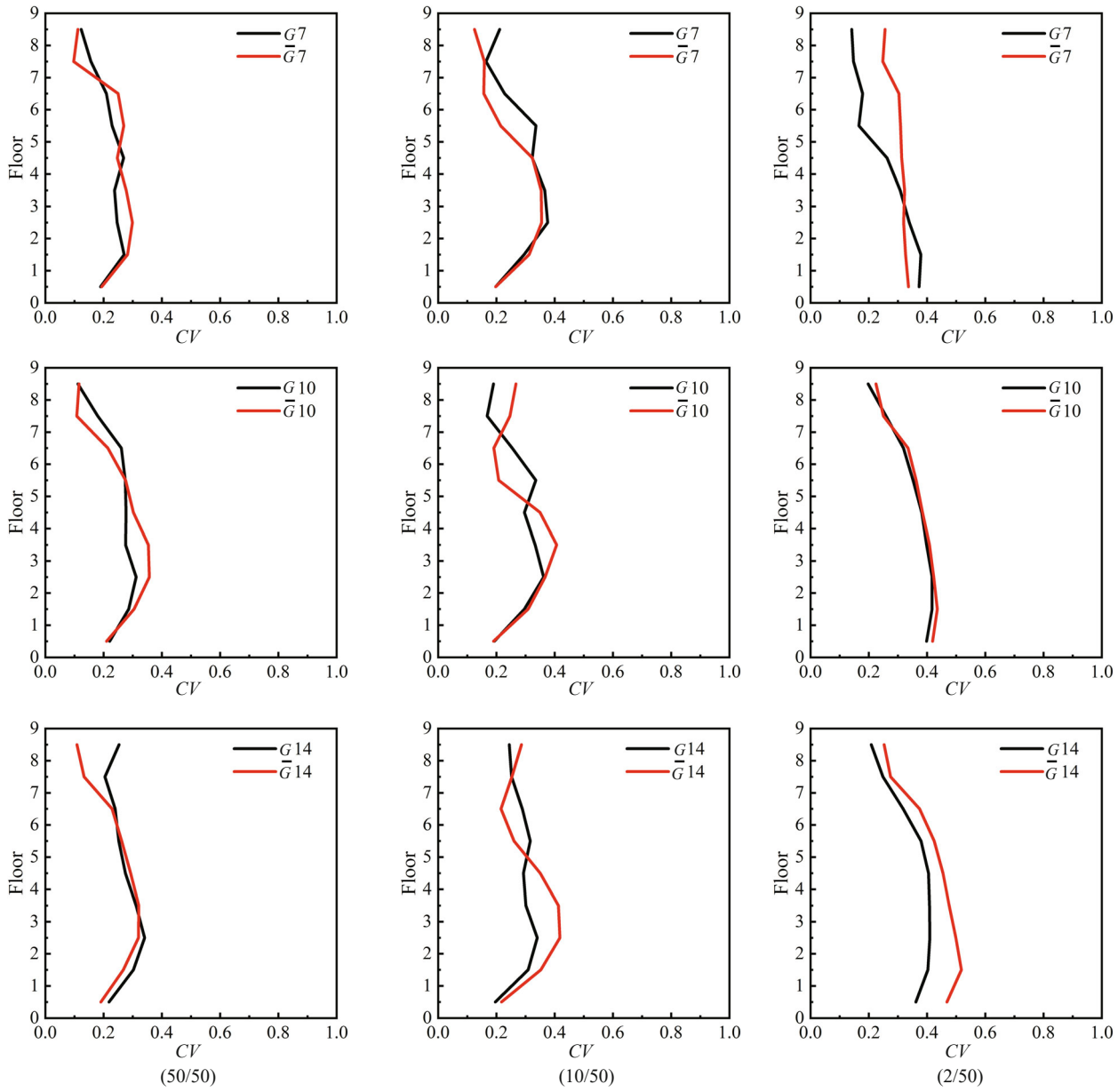

Fig. 9 ***CV*s of PIDR demands over heights of the 9-story structure under ground motion groups *Gi* ($\overline{G}i$) (*i* = 7, 10, 14) at 50/50, 10/50, and 2/50 hazard levels**

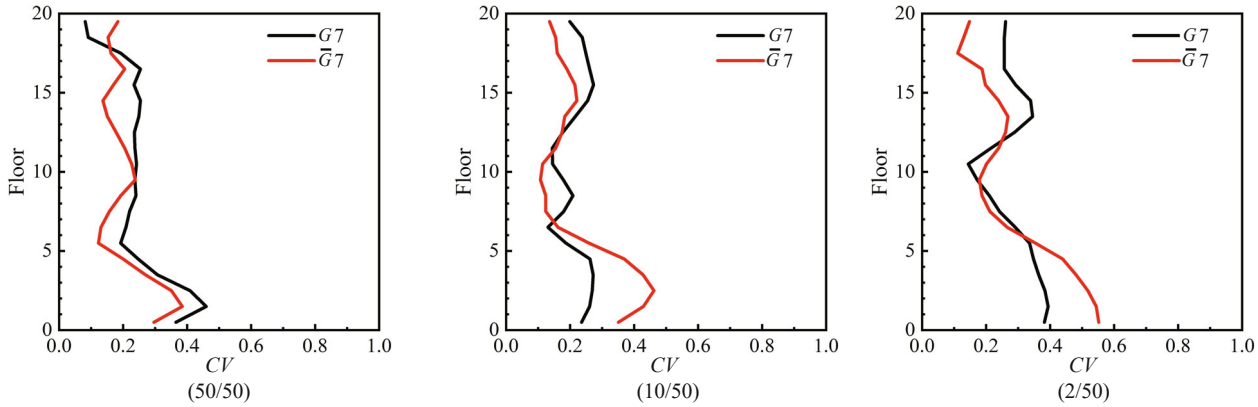

Fig. 10 ***CV*s of PIDR demands over heights of the 20-story structure under ground motion groups *Gi* ($\overline{G}i$) (*i* = 7, 10, 14) at 50/50, 10/50, and 2/50 hazard levels**

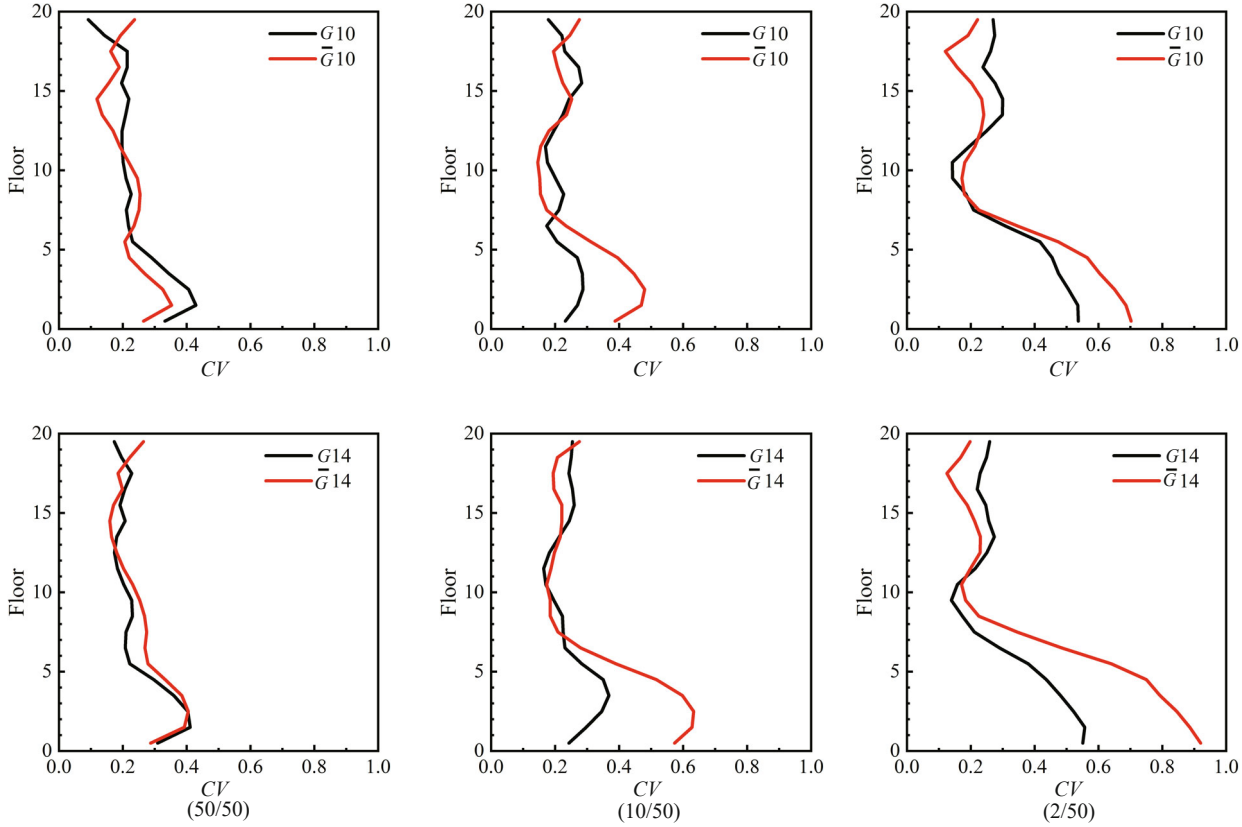

Fig. 10 Continued

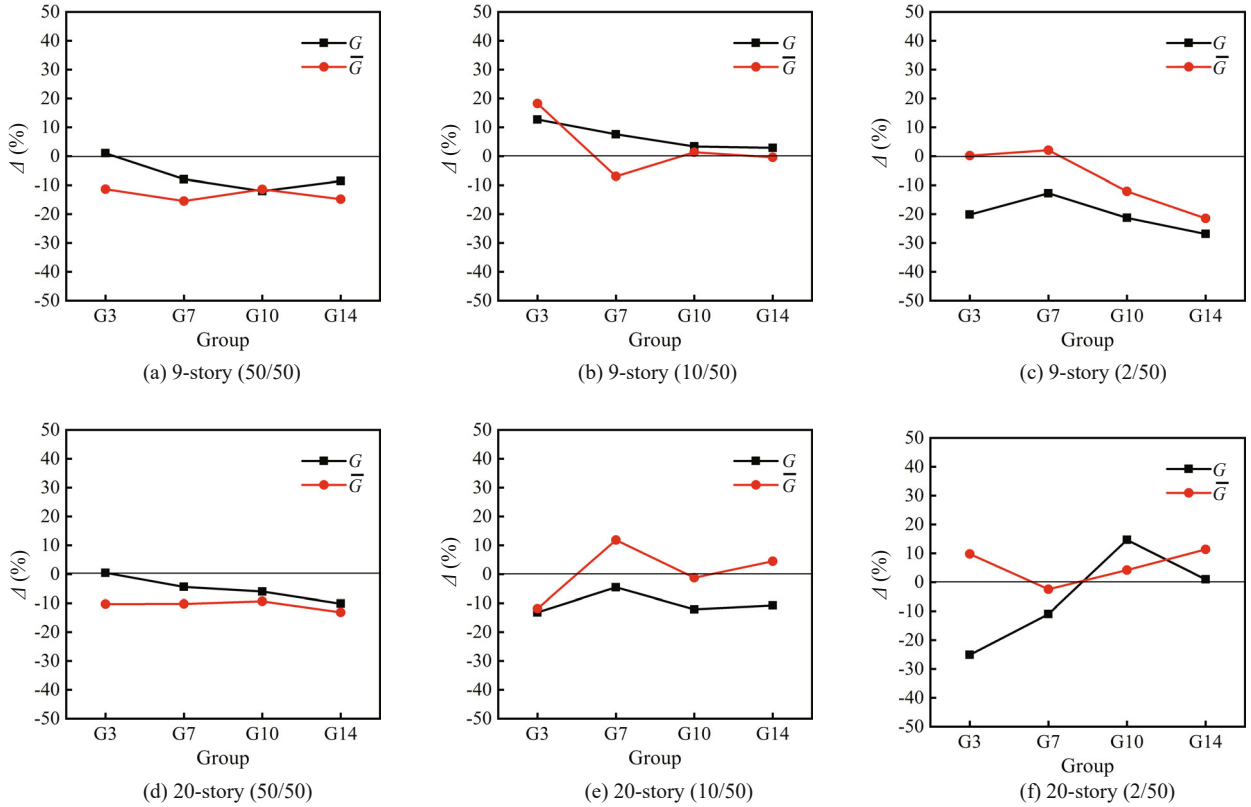

Fig. 11 Relative errors of MIDR demands for the 9-story and 20-story structures under ground motion groups *Gi* ($\overline{Gi}$) (*i* = 3, 7, 10, 14) at 50/50, 10/50, and 2/50 hazard

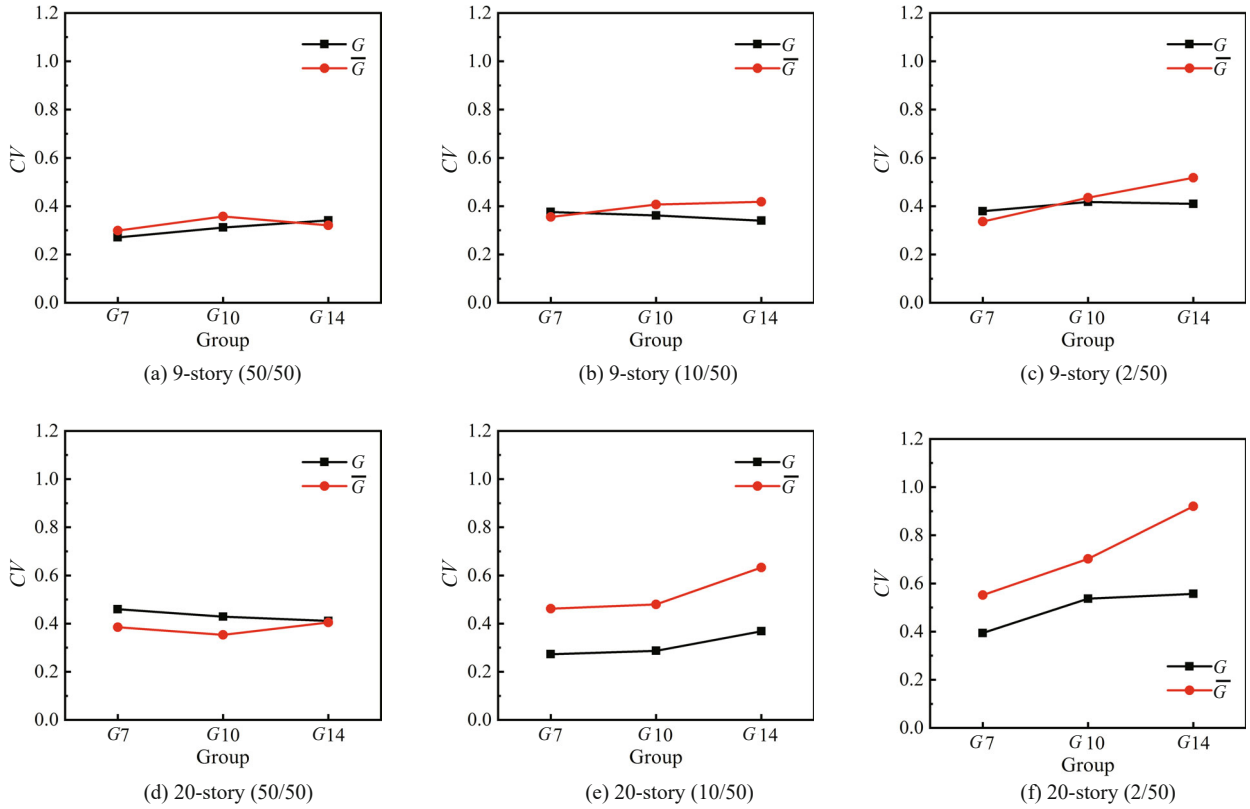

Fig. 12 Relative errors of MIDR demands for the 9-story and 20-story structures under ground motion groups *Gi* ($\overline{G}i$) (*i* = 7, 10, 14) at 50/50, 10/50, and 2/50 hazard

4 Conclusions

The main objective of selecting and scaling ground motions for time-history analysis is to accurately estimate structural mean EDPs and to reduce the variability of mean results with fewer records, especially for the seismic design of the real structures. In this study, a ground motion selection and modification method was proposed using the Newmark-Hall spectrum as the target spectrum. The Newmark-Hall spectrum has a perfect correlation with the structural responses of short, medium, and long-periods. For time history analysis of a real structure, when the Newmark-Hall spectra is used as the target spectra, the input records will be adaptive selected and scaled to the acceleration sensitive, velocity sensitive or displacement sensitive zones of the spectrum, according to the structural fundamental period.

The 9-story and 20-story steel moment-resisting frame structures, representing medium-period and long-period buildings, were used as examples. The potential feasibility for taking the Newmark-Hall spectrum as the target spectrum was verified. In nonlinear time-history analysis, based on a comparison of the N-HM and A-SM methods, the structural mean responses to the benchmark mean demands and the relative errors were present under seismic excitations at various seismic hazard levels. The main conclusions are summarized as follows:

(1) For the medium-period structure, i.e., 9-story structure, *SF*s of ground motions obtained by the N-HM method are generally larger than those derived from the A-SM method. However, the differences of *SF*s from both methods are reduced for the long-period structure, i.e., the 20-story structure. Thus, *SF*s are more likely to be controlled by spectral values in the velocity-sensitive regions for the 20-story structure whenever the Newmark-Hall spectrum or the acceleration spectrum is taken as the target spectrum.

(2) The N-HM and A-SM methods have a similar estimation accuracy of structural mean response. The absolute values of the relative errors of structural inter-story drift-ratio demands can be in an acceptable range, e.g., less than 20%. The accuracy is not sensitive to the structural dynamic characteristics, the required number of records (7 or 10), and the nonlinear degree of the structural response.

(3) The main advantage of the N-HM method is that it has a proper performance in reducing the variability of the structural responses. This performance is more significant for longer-period structures or structure with a more severe nonlinear response.

It is important to note that only the average responses of these buildings are considered in the present study, even though the probability distribution of EDPs and collapse probability of the buildings are as significant as the average responses. Thus, detailed investigations of the seismic probability response can be conducted in

future studies. In addition, there are some real near-fault ground motions in the record set representing the seismic hazard level with the 2% probability of exceedance in 50 years for the SAC Steel Project. However, in the present study, near-fault ground motions with forwarding directivity effects were removed during the selection of ground motions.

Data and Resources

Data used in this study can be found in the Pacific Earthquake Engineering Research Center Strong Motion Database at ngawest2.berkeley.edu (last accessed January 2019). Some or all data, models, or code generated or used during the study are available from the corresponding author by request.

Acknowledgement

This research is supported by the National Natural Science Foundation of Hebei Province under Grant No. E2020202038, and the National Natural Science Foundation of China under Grant No. 51778206.

References

ABAQUS (2012), *Online Documentation 6*, *12ed*, Dassault Systems, France.

ASCE 4-98 (2000), *Seismic Analysis of Safety-Related Nuclear Structures and Commentary*, American Society of Civil Engineers, Reston, Virginia, USA.

ASCE 7-10 (2010), *Minimum Design Loads for Buildings and Other Structures*, American Society of Civil Engineers, Reston, Virginia, USA.

Baker JW (2011), "Conditional Mean Spectrum: Tool for Ground-Motion Selection," *Journal of Structural Engineering*, **137**(3): 322–331.

Baker JW and Cornell CA (2006), "Spectral Shape, Epsilon and Record Selection," *Earthquake Engineering and Structural Dynamics*, **35**(9): 1077–1095.

Baker JW and Lee C (2017), "An Improved Algorithm for Selecting Ground Motions to Match a Conditional Spectrum," *Journal of Earthquake Engineering*, **22**(4): 708–723.

Beyer K and Bommer JJ (2007), "Selection and Scaling of Real Accelerograms for Bi-Directional Loading: A Review of Current Practice and Code Provisions," *Journal of Earthquake Engineering*, **11**(S1): 13–45.

Bommer JJ and Acevedo AB (2004), "The Use of Real Earthquake Accelerograms as Input to Dynamic Analysis," *Journal of Earthquake Engineering*, **8**(S1): 43–91.

Calvi GM, Rodrigues D and Silva V (2018), "A Redefinition of Seismic Input for Design and Assessment," in: Pitilakis K. (eds) *Recent Advances in Earthquake Engineering in Europe*, *Geotechnical, Geological and Earthquake Engineering*, vol 46. Chapter 3, Springer cham.

Campbell KW and Bozorgnia Y (2008), "NGA Ground Motion Model for the Geometric Mean Horizontal Component of PGA, PGV, PGD and 5% Damped Linear Elastic Response Spectra for Periods Ranging from 0.01 to 10 s," *Earthquake Spectra*, **24**(1): 139–171.

Carlton B and Abrahamson N (2014), "Issues and Approaches for Implementing Conditional Mean Spectra in Practice," *Bulletin of the Seismological Society of America*, **104**(1): 503–512.

Catalán A, Benavent-Climent A and Cahís X (2010), "Selection and Scaling of Earthquake Records in Assessment of Structures in Low-to-Moderate Seismicity Zones," *Soil Dynamics and Earthquake Engineering*, **30**(1–2): 40–49.

CEN (2005), *EN 1998-3*, *Eurocode 8*: *Design of Structures for Earthquake Resistance*, Brussels: European Committee for Standardization, Belgium.

Chen YB, Xu LJ, Zhu XJ and Liu H (2018), "A Multi-Objective Ground Motion Selection Approach Matching the Acceleration and Displacement Response Spectra," *Sustainability*, **10**(12): 4659.

Chopra AK (2004), "Estimating Seismic Demands for Performance-based Engineering of Buildings," *Proceedings of the 13th World Conference on Earthquake Engineering*, Vancouver B.C., Canada.

Cornell CA, Howells DA, Haigh IP and Taylor C (1971), "Probabilistic Analysis of Damage to Structures Under Seismic Loads," *Dynamic Waves in Civil Engineering*, 473–488.

CSA (2010), *Design Procedures for Seismic Qualification of Nuclear Power Plants*, *Standard CSA-N289*, *3-10*. Canadian Standard Association (CSA), Mississauga, Ontario, Canada.

DOE (2002), *Natural Phenomena Hazards Assessment Criteria*, *Standard DOE-STD-1023-2002*, U.S. Department of Energy, Washington D.C., USA.

FEMA 273 (1997), *NEHRP Guidelines for the Seismic Rehabilitation of Buildings*, Federal Emergency Management Agency, Washington D.C., USA.

Gupta A and Krawinkler H (1999), *Seismic Demands for Performance Evaluation of Steel Moment Resisting Frame Structures* (*SAC Task 5.4.3*), U.S.: Blume Earthquake Engineering Center, Stanford University, Palo Alto.

Hall WJ, Mohraz B and Newmark NM (1976), "Statistical Studies of Vertical and Horizontal Earthquake Spectra," *Nuclear Regulatory Commission Report*, U.S. Urbana, Illinois, NUREG-0003.

Haselton CB (2009), "Evaluation of Ground Motion Selection and Modification Methods: Predicting Median Interstory Drift Response of Buildings," *PEER Rep*,

Berkeley, CA: PEER, USA.

Kalkan E and Chopra AK (2010), "Practical Guidelines to Select and Scale Earthquake Records for Nonlinear Response History Analysis of Structures," *U.S. Geological Survey Open-File Report*.

Katsanos EI and Sextos AG (2017), "Structure-Specific Selection of Earthquake Ground Motions for the Reliable Design and Assessment of Structures," *Bulletin of Earthquake Engineering*, **16**(2): 583–611.

Katsanos EI, Sextos AG and Manolis GD (2010), "Selection of Earthquake Ground Motion Records: A State-of-the-Art Review from a Structural Engineering Perspective," *Soil Dynamics and Earthquake Engineering*, **30**(4): 157–169.

Kwong NS and Chopra AK (2017), "A Generalized Conditional Mean Spectrum and Its Application for Intensity-Based Assessments of Seismic Demands," *Earthquake Spectra*, **33**(1): 123–143.

Li Bo, Xie WC and Pandey MD (2016), "Newmark Design Spectra Considering Earthquake Magnitudes and Site Categories," *Earthquake Engineering and Engineering Vibration*, **15**(3): 519–535.

Lombardi L, De Luca F and Macdonald J (2019), "Design of Buildings Through Linear Time-History Analysis Optimising Ground Motion Selection: A Case Study for RC-MRFs," *Engineering Structures*, **192**: 279–295.

Mahmoud MH (2008), "QuakeManager: A Software Framework for Ground Motion Record Management, Selection, Analysis and Modification," *Proceedings of the 14th World Conference on Earthquake Engineering*, Beijing, China.

Malhotra PK (2011), "Seismic Response Spectra for Probabilistic Analysis of Nonlinear Systems," *Journal of Structural Engineering*, **137**(11): 1272–1281.

Marasco S and Cimellaro GP (2017), "A New Energy-Based Ground Motion Selection and Modification Method Limiting the Dynamic Response Dispersion and Preserving the Median Demand," *Bulletin of Earthquake Engineering*, **16**(2): 561–581.

McGuire RK (2004), *Seismic Hazard and Risk Analysis*, Earthquake Engineering Research Institute, Oakland, CA, USA.

Mergos PE and Sextos AG (2019), "Selection of Earthquake Ground Motions for Multiple Objectives using Genetic Algorithms," *Engineering Structures*, **187**: 414–427.

Miranda E and Aslani H (2003), "Probabilistic Response Assessment for Building Specific Loss Estimation," *Technical Report*, *Pacific Earthquake Engineering Research Center*, Berkeley, USA.

Miranda E and Ruiz-García J (2001), "Evaluation of Approximate Methods to Estimate Maximum Inelastic Displacement Demands," *Earthquake Engineering and Structural Dynamics*, **31**(3): 539–560.

Moschen L, Medina RA and Adam C (2019), "A Ground Motion Record Selection Approach Based on Multiobjective Optimization," *Journal of Earthquake Engineering*, **23**(4): 669–687.

Newmark NM, Blume JA and Kapur KK (1973), "Seismic Design Spectra for Nuclear Power Plants," *Journal of the Power Plants*, **99**(2): 287–303.

Newmark NM and Hall WJ (1969), "Seismic Design Criteria for Nuclear Reactor Facilities," *Proceedings of the Fourth World Conference on Earthquake Engineering*, B-4, 37–50, Santiago, Chile.

Newmark NM and Hall WJ (1982), "Earthquake Spectra and Design," *PEER Rep*, Berkeley, CA: PEER, USA.

Ohtori Y, Christenson RE, Spencer BF and Dyke SJ (2004), "Benchmark Control Problems for Seismically Excited Nonlinear Buildings," *Journal of Engineering Mechanics*, **130**(4): 366–385.

Padgett JE and DesRoches R (2007), "Sensitivity of Seismic Response and Fragility to Parameter Uncertainty," *Journal of Structural Engineering*, **133**(12): 1710–1718.

Palermo M, Silvestri S, Gasparini G and Trombetti T (2014), "A Statistical Study on the Peak Ground Parameters and Amplification Factors for an Updated Design Displacement Spectrum and a Criterion for the Selection of Recorded Ground Motions," *Engineering Structures*, **76**: 163–176.

PEER GMSM Working Group (2009), "Evaluation of Ground Motion Selection and Modification Methods: Predicting Median Inter-Story Drift Response of Buildings," *PEER Rep*, Berkeley, CA: PEER, USA.

Reyes JC and Kalkan E (2011), "Required Number of Records for ASCE/SEI 7 Ground Motion Scaling Procedure," *U.S.: Geological Survey Open-File Report*.

Reyes JC, Riaño AC, Kalkan E, Quintero OA and Arango CM (2014), "Assessment of Spectrum Matching Procedure for Nonlinear Analysis of Symmetric-and Asymmetric-Plan Buildings," *Engineering Structures*, **72**: 171–181.

Riddell R (2007), "On Ground Motion Intensity Indices," *Earthquake Spectra*, **23**(1): 147–173.

Riddell R and Garcia JE (2001), "Hysteretic Energy Spectrum and Damage Control," *Earthquake Engineering and Structural Dynamics*, **30**(12): 1791–1816.

Shome N, Cornell CA, Bazzurro P and Carballo JE (1998), "Earthquakes Records and Nonlinear Response," *Earthquake Spectra*, **14** (3): 469–500.

Somerville P, Smith NF, Punyamuthula S and Sun J (1997), "Development of Ground Motion Time Histories for Phase 2 of the FEMA/SAC Steel Project," *SAC Joint Venture*, *SAC/BD-97/04*, Sacramento, California, USA.

Theophilou A-A I (2019), "A Ground Motion Selection and Modification Method Through Stratified Sampling," *Bulletin of Earthquake Engineering*,**17**(2): 637–655.

Wang G (2011), "A Ground Motion Selection and Modification Method Capturing Response Spectrum

Characteristics and Variability of Scenario Earthquakes," *Soil Dynamics and Earthquake Engineering*, **31**(4): 611–625.

Wang G, Youngs R, Power M and Li ZH (2015), "Design Ground Motion Library: An Interactive Tool for Selecting Earthquake Ground Motions," *Earthquake Spectra*, **31**(2): 617–635.

Zhang R, Wang DS, Chen XY and Li HN (2020), "Weighted and Unweighted Scaling Methods for Ground Motion Selection in Time-history Analysis of Structures," *Journal of Earthquake Engineering*, **26**(6): 3148–3183.

Zhang YT, He Z and Yang YF (2017), "A Spectral-Velocity-Based Combination-Type Earthquake Intensity Measure for Super High-Rise Buildings," *Bulletin of Earthquake Engineering*, **16**(2): 643–677.